Spectral Observation of an Acyl-Enzyme Intermediate of Lipoprotein Lipase†

Camilo Rojas, Huei-Hsiang Wang, Chris R. Lively, William G. Gustafson, Leslie O. Schulz, and James T. McFarland*

Department of Chemistry, University of Wisconsin—Milwaukee, Milwaukee, Wisconsin 53201

Received June 16, 1988; Revised Manuscript Received January 25, 1989

ABSTRACT: There have been several studies indicating that hydrolysis reactions of fatty acid esters catalyzed by lipases proceed through an acyl-enzyme intermediate typical of serine proteases. In particular, one careful kinetic study with the physiologically important enzyme lipoprotein lipase (LPL) is consistent with rate-limiting deacylation of such an intermediate. To observe the spectrum of acyl-enzyme and study the mechanism of LPL-catalyzed hydrolysis of substrate, we have used a variety of furylacryloyl substrates including 1,2-dipalmitoyl-3-[(β-2-furylacryloyl)triacyl]glyceride (DPFATG) to study the intermediates formed during the hydrolysis reaction catalyzed by the enzyme. After isolation and characterization of the molecular weight of adipose LPL, we determined its extinction coefficient at 280 nm to quantitate the formation of any acyl-enzyme intermediate formed during substrate hydrolysis. We observed an intermediate at low pH during the enzyme-catalyzed hydrolysis of (furylacryloyl)imidazole. This intermediate builds early in the reaction when a substantial amount of substrate has hydrolyzed but no product, furylacrylate, has been formed. The acyl-enzyme has a λ_{max} = 305 nm and a molar extinction coefficient of 22 600 M^{-1} cm^{-1}; these parameters are similar to those for furylacryloyl esters including the serine ester. These data provide the first spectral evidence for a serine acyl-enzyme in lipase-catalyzed reactions. The LPL hydrolysis reaction is base catalyzed, exhibiting two pK_a values; the more acidic of these is 6.5, consistent with base catalysis by histidine. The biphasic rates for substrate disappearance or product appearance and the absence of leaving group effect indicate that deacylation of intermediate is rate limiting.

As part of a continuing program in the design and use of chromophoric reagents for the investigation of fatty acid metabolizing enzymes, we have reported the synthesis of 1,2-dipalmitoyl-3-[(β-2-furylacryloyl)triacyl]glyceride (DPFATG)[1] and its use in the investigation of the mechanism of bacterial lipase from *Pseudomonas fragi* (McFarland & Rojas, 1986). The Michaelis constant for this substrate is comparable to that of tripalmitin, indicating that DPFATG is a good substrate. The rate of bacterial lipase catalyzed hydrolysis is faster at more basic pH values, while the binding constant is pH independent. These results are in agreement with a paper on another bacterial lipase (Sugiura, 1984) and are consistent with the notion that catalysis of triacylglyceride hydrolysis is limited by the rate of acylation of enzyme, assuming that an acyl-enzyme mechanism applies to this enzyme.

On the other hand, studies on mammalian lipoprotein lipase (LPL) from milk indicate that there is an acyl-enzyme intermediate whose deacylation is rate limiting (Burdette & Quinn, 1986). This investigation confirms earlier studies using benzeneboronic acid as an inhibitor that also suggest such a serine acyl-enzyme intermediate (Vainio et al., 1982). A recent paper has suggested the location of a possible active site diad of serine and histidine in the LPL sequence (Reddy et al., 1986). However, there has been no spectral demonstration of an acyl-enzyme with any of the lipases; furylacryloyl substrates are ideal for such a demonstration because their ester and amide derivatives, including the acyl-enzyme intermediates of a serine protease, have been studied by electronic spectroscopy (Bernhard et al., 1965). The technique of spectral identification of the intermediate is ideally suited to LPL investigation because the lability of the enzyme makes isolation and chemical analysis difficult.

Finally, we have chosen to search for an acyl-enzyme intermediate with the adipose enzyme because the enzyme is available in large amounts from this tissue, and the physiological role of adipose LPL is clear. Furthermore, there seems to be a great deal of similarity among mammalian LPLs (Iverius & Ostlund-Lindqvist, 1986; Ostlund-Lindqvist, 1979), so that observations made on one enzyme should apply to others. The purification and molecular weight determination of rat adipose LPL have been reported (Parkin et al., 1982); the enzyme has also been characterized by antibody specificity (Olivecrona & Bengtsson, 1983). We report enzyme purification, molecular weight determination, and determination of the 280-nm extinction coefficient. In addition, we report mechanistic data with the chromophoric furylacryloyl substrates that suggest the presence of an acyl-enzyme intermediate and rate-limiting deacylation. We also report the pH dependence of the steady-state parameters for the hydrolysis of DPFATG.

Materials and Methods

Preparation of DPFATG. The preparation has been described previously (McFarland & Rojas, 1986). DPFATG monomer is prepared by sonication of DPFATG in the buffer of choice followed by gel exclusion chromatography on Bio-Gel P-30; the monomeric substrate is eluted from this column with approximately the same R_f value as potassium ferricyanide.

Preparation and Characterization of Mammalian Lipoprotein Lipase. Mammalian lipoprotein lipase was isolated from rat adipose tissue. The procedure was based on a previous paper (Parkin et al., 1982). Briefly, rats were fed 5% glucose solutions 48 h before sacrificing. Adipose tissue deposits were

† This research was supported by Grant GM 32504-01 from the National Institutes of Health.

* Author to whom correspondence should be addressed.

[1] Abbreviations: DPFATG, 1,2-dipalmitoyl-3-[(β-2-furylacryloyl)-triacyl]glyceride; LPL, lipoprotein lipase; PC, phosphatidylcholine; FA, β-2-furylacryloyl.

0006-2960/89/0428-4475$01.50/0

placed in ice-cold Tris buffer (pH 7.4, 20 mM, 0.15 M NaCl) and homogenized with a mortar and pestle; sand was added to aid the homogenizing procedure. The homogenate was centrifuged in a desk-top International Clinical centrifuge Model CL for 20 min, and the supernatant containing lipoprotein lipase was added to an affinity column (heparin–Sepharose 4B) at 4 °C. Lipoprotein lipase as well as other lipases present in the supernatant binds to heparin at a low NaCl concentration (0.15 M), but they can be separated selectively by elution with a salt gradient. The column was washed with several (2–3) column volumes of Tris buffer (20 mM, pH 7.4, in 20% glycerol, which is known to stabilize LPL) containing increasing NaCl concentrations (0.3, 0.75 M). Lipoprotein lipase was eluted from the column when buffer containing 1.5 M NaCl was applied. Absorbance readings (280 nm) of the fractions eluting at 1.5 M NaCl were recorded, and those fractions containing protein were assayed for hydrolytic activity with DPFATG. The enzyme was stored in liquid nitrogen until further use. The isolated enzyme was pure as determined by 10% SDS–polyacrylamide slab gel electrophoresis. The extinction coefficient of the enzyme was determined from the total protein concentration (Lowry) or from the weight of protein residue after lyophilization in ammonium carbonate. The molecular weight of the protein was determined from a plot of retention time vs molecular weight from the SDS–PAGE chromatogram of LPL and standards. We have employed the standard radioactive assay for determination of the activity of adipose LPL; this method relies upon the extraction of radioactively labeled [^{14}C]oleic acid from the enzyme-catalyzed hydrolysis of triolein as a substrate (Iverius & Ostlund-Lindqvist, 1976).

Steady-State Kinetic Experiments with Mammalian Lipoprotein Lipase: pH Dependence. The experimental procedure was the same as that outlined for the steady-state kinetic experiments with bacterial lipase and monomeric solutions of DPFATG (McFarland & Rojas, 1986). The method consists of determination of the rate of disappearance of the DPFATG observed at 312 nm, the wavelength at which the maximum difference extinction coefficient (12 500 M^{-1} cm^{-1}) between DPFATG and furylacrylate anion is observed. Enzyme concentration was determined from the 280-nm absorbance and the extinction coefficient (90 386 M^{-1} cm^{-1}). The final concentration of enzyme was in the range 40–60 nM for different pH values, but all assays at a given pH had the same enzyme concentration. The concentration of substrate was varied from about 8 to 47 μM at each pH. The determination of V_{max} and K_m values was made from Lineweaver–Burk plots; each plot included values corresponding to at least five different determinations of rate of enzyme-catalyzed hydrolysis vs concentration of DPFATG. The value of the first-order rate constant, k_{cat}, is the value of V_{max} divided by the enzyme concentration at each pH. Buffers used were acetate (pH 4.5 and 5.5), imidazole (pH 7.0 and 7.5), phosphate (pH 7.5), Tris (pH 8.5), and glycine (pH 9.6 and 10.5). The concentration of each buffer was 0.020 M; the ionic strength of each solution was kept constant at 0.1 M by adding the necessary amounts of NaCl. To determine that rate changes in going from one pH to another are not due to a buffer effect, the rate for the hydrolysis reaction was determined in two different buffers at the same pH for several pH values: imidazole and phosphate at pH 6.0, Tris and imidazole at pH 8.0, and Tris and glycine at pH 9.0. The rates obtained at the same pH for the two buffers at pH 6.0 and 9.0 were essentially the same. At pH 8.0, the rate of the reaction in imidazole buffer is 1.8 times greater than the rate obtained in Tris buffer. The different rates are most likely due to additional base hydrolysis coming from imidazole, which is essentially unprotonated at pH 8.0 ($pK_{a,im}$ = 6.95). Finally, to assure that we are seeing enzymatic catalysis, we performed another control experiment in which enzyme concentration was doubled while substrate concentration was kept the same. When the enzyme concentration was doubled, the rate also doubled, so we can confidently say that the reaction is first order with respect to enzyme concentration.

Leaving Group Effect. Rate constant values were determined for LPL-catalyzed hydrolysis of DPFATG, (furylacryloyl)imidazole, and ethyl furylacrylate ester in acetate buffer (pH 5.5, 0.050 M, NaCl 0.050 M). The steady-state experiments were carried out as outlined in the previous section. (Furylacryloyl)imidazole was synthesized as reported previously (Schonbaum et al., 1961). Hydrolysis of (furylacryloyl)imidazole was followed at 340 nm, where ϵ = 27 000 M^{-1} cm^{-1} (Bernhard et al., 1965). The synthesis of ethyl furylacrylate ester involves the same steps as the synthesis of DPFATG, except that in the esterification reaction ethanol was used as both solvent and esterifying agent. The electronic spectra of ethyl furylacrylate ester and DPFATG are the same, so hydrolysis of the ethyl ester was monitored in the same manner as for DPFATG. Chemical hydrolysis of (furylacryloyl)imidazole and DPFATG was carried out at different concentrations of each substrate while the pH was kept constant and then the hydroxide ion concentration was varied while the substrate concentration was kept the same. In the case of DPFATG, the hydroxide ion concentrations were much higher (0.1 and 0.2 M) than for (furylacryloyl)imidazole (in the range 10^{-4}–10^{-9} M). The higher hydroxide ion concentrations were needed for DPFATG because this substrate does not hydrolyze significantly at pH <12.

Observation of Acyl-Enzyme Intermediate. Lipoprotein lipase was concentrated in a small-diameter dialysis tubing with poly(ethylene glycol) at 4 °C. When the volume of the solution inside the tubing was about 0.5 mL, acetate buffer (pH 5.0, 0.1 M) was added to the solution inside the tubing and the protein was concentrated once again. This procedure was repeated three times to ensure enzyme equilibration with buffer. The final volume of enzyme solution was adjusted to 1.0 mL. After LPL was concentrated, the electronic spectrum of the enzyme was measured. Only an estimate of the enzyme concentration is possible because the protein spectrum has a significant amount of light scattering. The acylating agent, (furylacryloyl)imidazole, was added, in an approximately 1:1 concentration ratio for LPL and (furylacryloyl)imidazole. The reaction was carried out in a Hewlett-Packard 8451-A diode array spectrophotometer at 10 °C. An electronic spectrum was obtained 15 s after mixing and then at 1-min time intervals for 4 min. After this time, spectra were measured at longer time intervals since absorbance change with respect to time is smaller at longer times during the reaction.

Data Analysis. Difference spectra were obtained by subtracting from the observed spectra the spectrum of protein scattering, the spectrum of substrate remaining, and the spectrum of product formed at different times during the reaction. The concentrations of substrate and of product formed were determined from absorbances and the corresponding extinction coefficients at wavelengths where substrate or product is the only species showing absorbance changes. The wavelengths used for (furylacryloyl)imidazole and furylacrylic acid were 360 nm (ϵ = 19 497 M^{-1} cm^{-1}) and 280 nm (ϵ = 14 295 M^{-1} cm^{-1}), respectively. Since there is a small substrate absorbance at 280 nm, the concentration of product

was determined after determination of substrate concentration. Furthermore, since no other species absorbs at 360 nm, the substrate concentration is our most reliable determination. Accordingly, our difference spectra consist of product and intermediate since these are mechanistically interpretable and require a minimum of spectral manipulation. It was assumed that the spectrum of protein does not change during the reaction.

Determinations of acylation (k_2) and deacylation (k_3) rate constants were made from the time course data. The rate constant for the faster process, acylation, is obtained by plotting the logarithm of the difference between the value of the concentration of substrate at a particular time and the value of the concentration of substrate extrapolated from the linear portion of the plot against time for the early part of the reaction. The graphical method only provides a reliable estimate of the acylation rate constant. The rate constant for the slower process, deacylation, cannot be obtained directly from the slower region in the plot of absorbance vs time because the experiment does not involve a steady-state situation. The slow region in the plot corresponds to a mixture of zero- and first-order conditions since the concentrations of enzyme and substrate used for this experiment are of comparable magnitude. To obtain an estimate of the rate constant for deacylation, we used a kinetic simulation of the changes of concentration as a function of time for substrate, intermediate, and product after the burst reaction. The kinetic simulation was obtained by numerical integration of rate equations that include a single intermediate whose formation approximates k_2, the value obtained for acylation by the graphical method. An estimate of k_3, the rate constant for deacylation, was obtained from the best fit of the observed change of concentration with time. The concentration of active enzyme, k_2, and k_3 were varied to provide the best fit to the time course observed for product disappearance. If we compare the active-site concentration from the best fit to the kinetic data with the concentration of LPL determined from the extinction coefficient, we estimate that the fractional activity is 60%. The correspondence between the simulated and the observed data indicates that we are observing a furylacryloyl-LPL intermediate similar to that observed for the hydrolysis of (furylacryloyl)imidazole catalyzed by chymotrypsin.

Results

We have purified rat adipose LPL by affinity chromatography on heparin–Sepharose. We find that there are several fractions which show activity for hydrolysis of DPFATG; however, it is the fraction that elutes with 1.5 M NaCl which exhibits the correct molecular weight, pH dependence typical of other mammalian LPLs, and activation with apo C-II. We have performed PAGE on this fraction, and we find a molecular weight of 56 000 as reported previously (Parkin et al., 1982) with little evidence of antithrombin III contamination (Parkin et al., 1982). This molecular weight is also similar to that of the bovine milk enzyme (Kinnunen, 1977). There is a high degree of homology between mammalian LPLs; the latter assertion is supported by comparison of the amino acid composition of the bovine milk LPL (Iverius & Ostlund-Lindqvist, 1986) with the sequence of th e human plasma enzyme (Ostlund-Lindqvist, 1979). We have determined the extinction coefficient of adipose LPL by measurement of the total protein concentration either by Lowry determination or by weighing the protein residue after lyophilization in ammonium bicarbonate. The resulting $\epsilon_{280} = 90\,386\ M^{-1}\ cm^{-1}$ agrees well with the equivalent number for the bovine milk enzyme (Olivecrona et al., 1982). The comparison of the specific activity based on the radioactive assay and the molar concentration of the enzyme (380 μmol min^{-1} mg^{-1}) with the specific activity of the milk enzyme (480 μmol min^{-1} mg^{-1}) (Olivecrona et al., 1982) and previous papers (Parkin et al., 1982) on the rat adipose enzyme (280 μmol min^{-1} mg^{-1}) provides us with confidence that our enzyme preparation contains active enzyme. The enzyme activity increased 7-fold in the presence of apo C-II, indicating that the enzyme we have isolated is LPL.

We have followed the kinetic course of hydrolysis of (furylacryloyl)imidazole in the presence of enzyme at a concentration comparable to substrate to observe formation of acyl-enzyme intermediate. This experiment was carried out at pH 5 under buffer and substrate conditions similar to those used previously to observe acylchymotrypsin (Coll et al., 1982); this slows the reaction, permitting spectral determination at higher signal to noise ratio than is possible on the stopped-flow time scale. This is important because LPL has been isolated at relatively low concentration. Figure 1 shows the result of this study along with the results of a similar experiment with the *P. fragi* enzyme. In the latter case, acylation is the rate-limiting step, so there would be little accumulation of acyl-enzyme intermediate. Notice that the bacterial lipase catalyzed reaction exhibits isosbestic behavior (Figure 1D), indicating formation of furylacrylate anion from hydrolysis of (furylacryloyl)imidazole. On the other hand, the rat adipose tissue LPL catalyzed hydrolysis proceeds without observation of an isosbestic point (Figure 1); we have shown the early stages (Figure 1A) of the reaction separated from the longer time course (Figure 1B) to emphasize the clear lack of isosbestic point. This suggests the presence of a third species, acyl-enzyme, during LPL catalysis of (furylacryloyl)imidazole hydrolysis. Figure 2A (lower trace) Figure 2C show the kinetically biphasic disappearance of starting material, (furylacryloyl)imidazole, consistent with the hypothesis that acyl-enzyme is formed during the reaction. The appearance of product shows a lag phase [Figure 2A (upper trace) and Figure 2B] during the same time interval as the rapid step observed for the disappearance of substrate (Figure 2C). These data indicate that an intermediate must be formed early in the reaction (between 0 and 400 s) since no product is produced during this period while approximately 1 enzyme equivalent of substrate is hydrolyzed.

To analyze the time dependence of the spectrum of intermediates and product formed during LPL-catalyzed hydrolysis shown in Figure 1, we have subtracted the absorbance and light scattering of enzyme [Figure 1C (bottom spectrum)] and the absorbance of substrate to produce Figure 3, which shows the time dependence of intermediate and product produced during hydrolysis of (furylacryloyl)imidazole. The substrate spectrum was removed by determining the concentration of substrate at 360 nm, where only it would be expected to absorb [(furylacryloyl)chymotrypsin has no absorbance at this wavelength]; the concentration was then used to determine the amount of substrate spectrum to remove for any time point. Figure 3A shows the electronic spectrum of an intermediate (λ_{max} = 305 nm) produced at short times during the rapid reaction of substrate or the lag in production of product. This spectrum is very similar to the spectrum of furylacrylic esters, e.g., the ethyl ester or glycerol ester (306-nm λ_{max}). Notice the production of furylacrylate product in Figure 3B at times longer than the 400-s "burst" reaction; the 305-nm spectrum of the intermediate observed during the lag phase for product continually shifts toward the 298-nm λ_{max} of furylacrylate product.

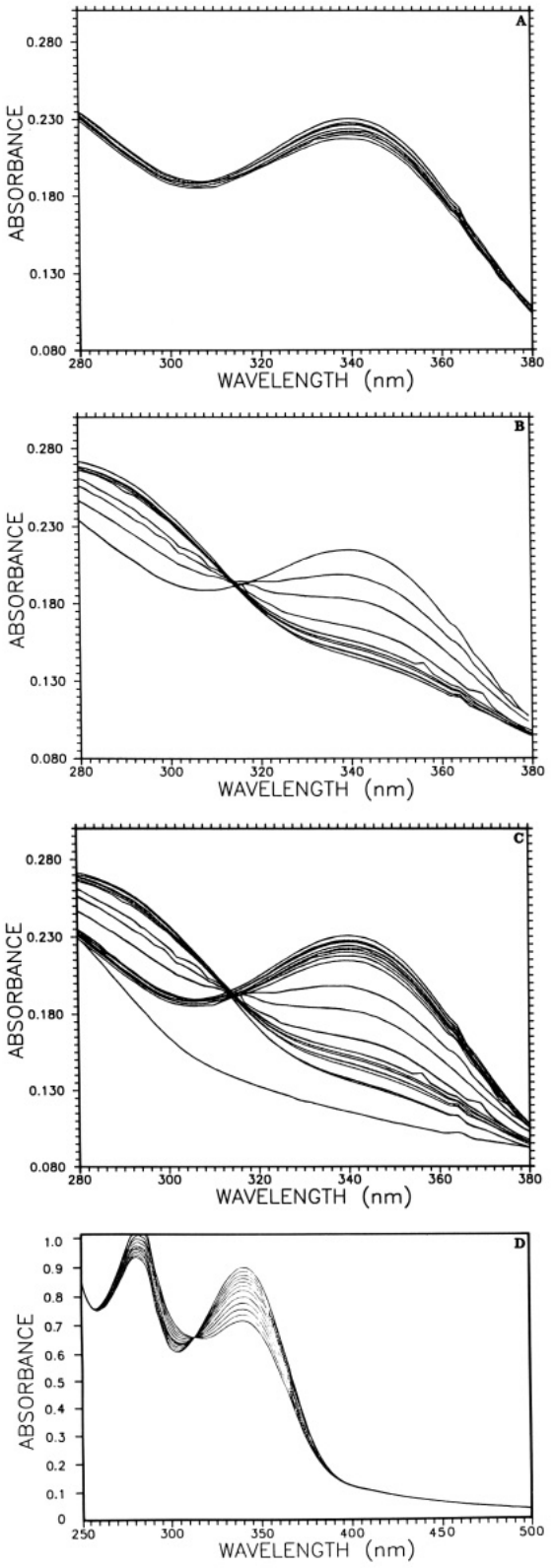

FIGURE 1: Time dependence of the LPL-catalyzed hydrolysis of FA-imidazole. [LPL] = 1.0×10^{-6} M; [FA-imidazole] = 5.0×10^{-6} M; 0.5 M acetate buffer, pH 5.0. (A) 75, 105, 135, 195, 225, 255, 380, 620, and 860 s. (B) 1340, 3802, 6202, 11 002, 12 396, 12 996, 13 596, 14 196, 14 796, 15 996 s. (C) (A) + (B) + 18 396, 18 996, and 0 s. (D) Bacterial lipase [lipase] = 6×10^{-6} M, [FA-imidazole] = 30×10^{-6} M, 0.5 M acetate buffer, pH 5.0.

Figure 4 shows a kinetic simulation of the disappearance of starting material, FA-imidazole, the formation and breakup of acyl-enzyme intermediate with absorbance at 305 nm, and the appearance of furylacrylate anion product; the data for disappearance of starting material and appearance of product

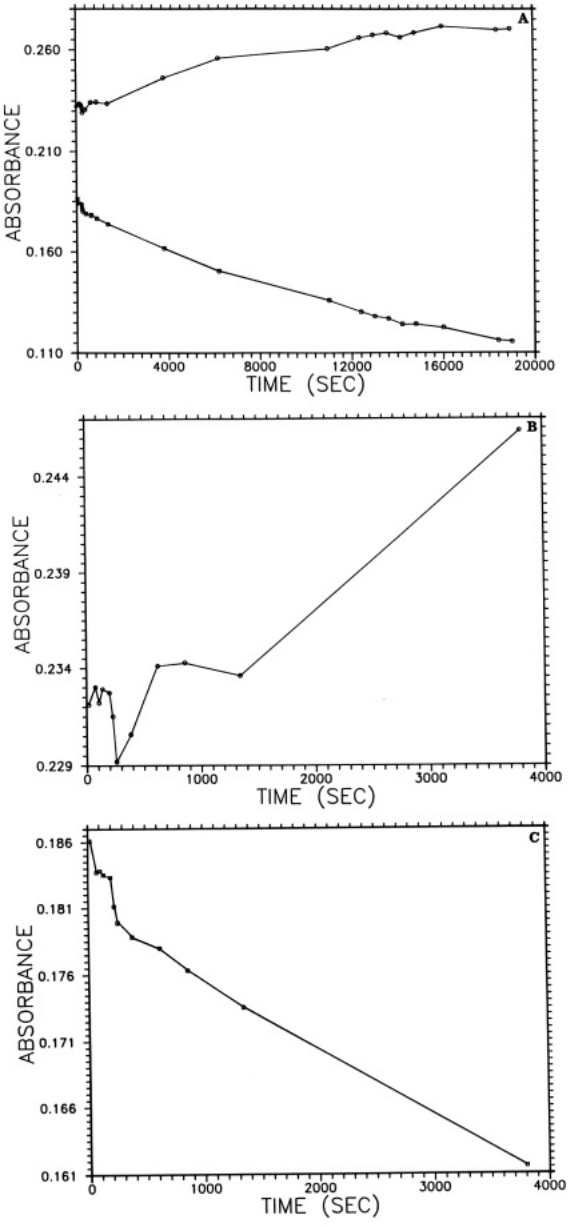

FIGURE 2: Time dependence of the substrate and product absorbances during LPL-catalyzed FA-imidazole hydrolysis. (A) Entire time course. For buffer conditions see Figure 1. (Upper trace) Product appearance (A_{280}); (lower trace) substrate disappearance (A_{360}). (B) Initial time course for product appearance (A_{280}). (C) Initial time course for substrate disappearance (A_{360}).

and intermediate are superimposed on the kinetic simulation. This simulation was obtained by numerical integration of the rate equations involving a single acyl-enzyme intermediate (Scheme I), whose formation and breakup follow the kinetic rate constants observed during adipose LPL catalyzed hydrolysis of FA-imidazole. The acylation rate constant was estimated directly from the first-order disappearance of starting material, but under the concentration conditions we have employed, the second rate process involves some turnover of enzyme, resulting in a rate process between first and zero order. Therefore, the deacylation rate constant could only be determined by comparison of observed data with calculations from our numerical integration. The simulation is consistent with acylation and deacylation rate constants of 1.2×10^{-2} and 5×10^{-4} s^{-1}, respectively. The absorbance change at 305 nm compared with the intermediate concentration predicted in the kinetic simulation shown in Figure 4 provides us with a rough estimate of the fractional activity of adipose LPL, 60%.

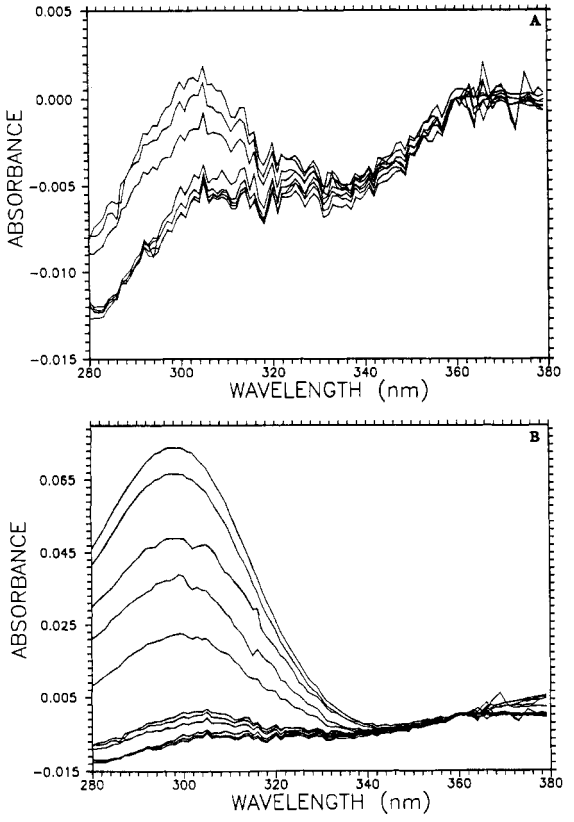

FIGURE 3: Time dependence of intermediate and product appearance. The spectra result from subtraction of enzyme and substrate absorbance from data in Figure 1. (A) 75, 135, 195, 225, 380, 620, 860, and 1340 s. (B) (A) + 3802, 6202, 11002, 14796, and 18996 s.

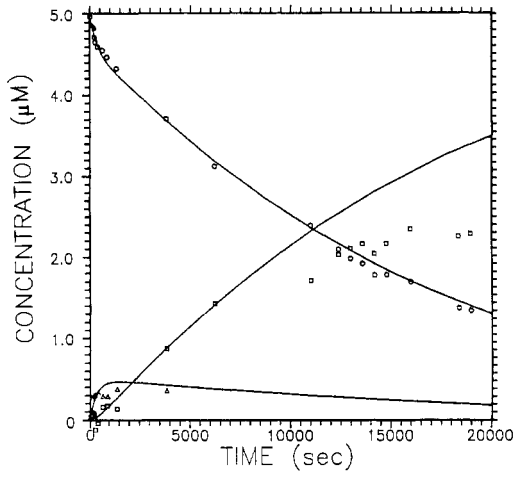

FIGURE 4: Comparison of observed and theoretical data for the rate of LPL-catalyzed FA-imidazole hydrolysis. Observed data are derived from the kinetic data shown in Figure 1 and the ϵ_{360nm} = 19497 for substrate (○) and ϵ_{280nm} = 17544 for product (□). The concentration of acyl-enzyme (△) was estimated by subtracting the concentration of enzyme, substrate, and product from the data of Figure 1. Theoretical data were calculated from the mechanism of Scheme I by using numerical integration of the rate expression; product inhibition was added, and the following rate and equilibrium constants were used: K_1 = 16 μM; k_2 = 1.2 × 10^{-2} s^{-1}; k_3 = 5.5 × 10^{-4} s^{-1}; K_4 = 1 μM; [S] = 5 μM; [E] = 0.6 μM.

A more accurate determination will be possible when we are able to increase the enzyme concentration so that it is in excess of substrate and no product results from enzyme turnover; at that time the determination can be made from hydrolysis to a product, FA acid anion, whose extinction coefficient is known.

To confirm the validity of our model for describing the data we present, we have simulated the spectral data of Figure 3 using the concentrations of starting material, intermediate acyl-enzyme, and product from our kinetic simulation along with the spectra of each of these species. The excellent correspondence (data not shown) between the simulated and observed data indicate that we are observing a furylacryloyl-enzyme intermediate.

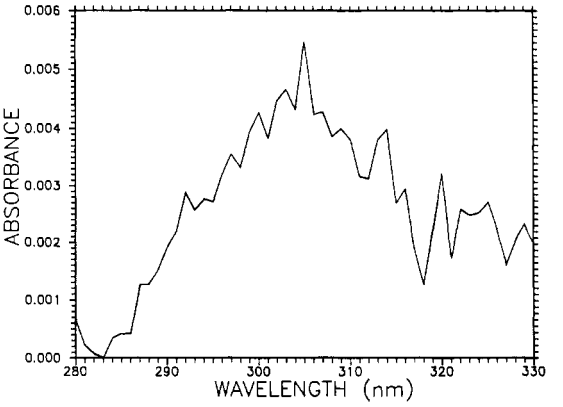

FIGURE 5: Spectrum of acyl-enzyme at 225 s.

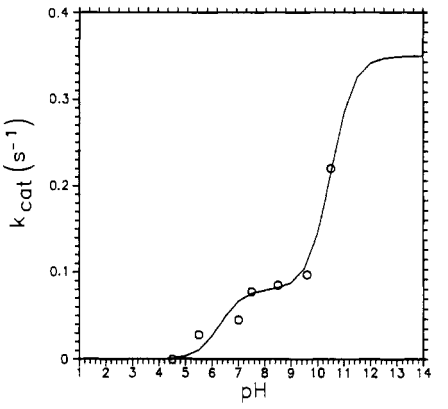

FIGURE 6: pH dependence of k_{cat} for the LPL-catalyzed hydrolysis of DPFATG. [E] = 40–60 nM; [S] = 8–47 μM. Buffers were 0.02 M containing 0.1 M NaCl as an ionic strength buffer; pH 4.5–5.5 acetate, pH 7.0–7.5 imidazole, pH 7.5 phosphate, pH 8.5 Tris, pH 9.5–10.5 glycine. The solid line represents the best fit to two well-separated ionic equilibria with pK_1 = 6.3 and pK_2 = 10.5.

Finally, the spectrum of the acyl-enzyme intermediate produced during the product lag phase at 225 s is shown in Figure 5; notice the 305-nm λ_{max} is similar to that observed for acylchymotrypsin but shows a normal ester spectrum with no red shift. These data constitute the first spectral evidence for such an acyl-enzyme intermediate in LPL-catalyzed hydrolysis reactions.

Figure 6 shows the pH dependence of the LPL-catalyzed hydrolysis of DPFATG; note the apparent base catalysis of V_{max} with a pK_a value of 6.3 followed by a second increase in V_{max} at very basic pH values. This is similar to the reported behavior of other mammalian LPLs (Bengtsson & Olivecrona, 1982), except that the two-step titration curve we observe is not as apparent. For the bovine milk enzyme, a continual slow increase in V_{max} as a function of pH is observed (Bengtsson & Olivecrona, 1982). It is clear that the pH dependence we observe is not the result of a single pH titration of one acid–base residue. It appears that with our chromophoric substrate the dependence of the rate parameters is sufficiently precise to permit resolution into two base-catalyzed processes. Table I shows the pH dependence of the K_m and V_{max}.

To test our hypothesis that LPL follows base-catalyzed nucleophilic catalysis with rate-limiting deacylation, we have

Table I: pH Dependence of the Steady-State Kinetic Parameters for the White Adipose LPL Catalyzed Hydrolysis of DPFATG

pH	$K_m \times 10^5$ (M)	$k_{cat} \times 10^2$ (s^{-1})
4.5		0
5.5	1.7 ± 0.95	2.8 ± 0.6
7.0	0.5 ± 0.07	4.5 ± 0.2
7.5	0.3 ± 0.18	7.7 ± 0.6
8.5	1.6 ± 0.33	8.5 ± 0.5
9.6	0.2 ± 0.01	9.7 ± 0.1
10.5	0.5 ± 0.04	22 ± 1.0

Scheme I

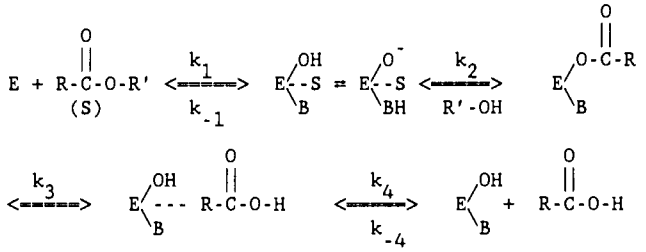

performed an experiment designed to identify the rate-limiting step. We have examined the leaving group effect upon k_{cat} at acidic pH. The acidic pH value permits us to examine the rate of hydrolysis of FA-imidazole, which is subject to rapid hydrolysis above pH 5. Values of k_{cat} for the LPL-catalyzed hydrolysis of the three substrates are 0.064 s^{-1} for DPFATG, 0.041 s^{-1} for FA-methyl ester, and 0.104 s^{-1} for FA-imidazole; notice that k_{cat} is nearly the same for the LPL-catalyzed hydrolysis of both the ethyl and glycerol esters (DPFATG) of furylacrylic acid as well as for (furylacryloyl)imidazole. We have also compared the rates of the chemical hydrolysis of the three substrates to the enzyme-catalyzed rates; although the bimolecular rate constants for hydrolysis of the two esters by hydroxide are similar, the equivalent rate constant for (furylacryloyl)imidazole is 5 orders of magnitude larger. These data indicate that the leaving group has little to do with the rate-limiting process; this indicates that the rate-limiting step is deacylation.

Discussion

Our mechanistic conclusions are summarized in Scheme I. Enzyme forms a noncovalent Michaelis complex, followed by acylation with furylacrylic acid to yield an acyl-enzyme intermediate. These experiments represent the first time the spectrum of such an intermediate has been observed during LPL-catalyzed hydrolysis; this intermediate has its λ_{max} = 305 nm (Figure 3). This λ_{max} = 305 nm is typical of furylacryloyl esters including those of serine (Table II); furthermore, this is nearly the same absorbance maximum as observed for α-chymotrypsin, strongly suggesting that the intermediate is a serine acyl ester of furylacrylic acid. However, acyl-chymotrypsin (λ_{max} = 320 nm) (Bernhard et al., 1965) shows a red shift observed upon comparison with normal furylacryloyl esters; the LPL acyl-enzyme shows no such red shift.

Results of our experiments indicate that the rate-limiting step is deacylation of acyl-enzyme, k_3. There is no leaving group effect in the three substrates we have studied; the rates of hydrolysis of the glycerol and ethyl esters of furylacrylic acid as well as of FA-imidazole are identical within experimental error.

The pH data establish that the rate-limiting step of deacylation is base catalyzed with a pK_a = 6.3 observed for the base catalyst. Most serine proteases exhibit base catalysis of V_{max} with approximately the same pK_a value as observed for the LPL-catalyzed hydrolysis of DPFATG; histidine's imidazole provides the base catalyst in serine proteases similar to α-chymotrypsin (Walsh, 1979). These facts point to histidine's imidazole as the base catalyst. Recent covalent labeling experiments have located an active-site peptide containing both serine and an adjacent histidine similar to the identification of such a diad of catalytic groups containing serine and histidine in other serine proteases (Walsh, 1979). At basic pH values a second ionization is observed; we are unable to determine the pK_a value for this second ionic group because we cannot reach the asymptote due to enzyme lability. It is possible that the direct removal of proton from the active-site serine is responsible for this second ionization. If this is the case, some fraction of serine protons are removed by the partition with the imidazole; this fraction is determined by the pK_a value of imidazole and the pK_a of serine at the active site. At more basic pH, protons remaining on serine may be removed directly from serine as the pH moves through the serine pK_a. Of course, the nucleophilic reactivity of serine is directly proportional to the fraction in the basic unprotonated form.

Table II: Electronic Spectral Properties of Furylacryloyl Esters and Amides

compound	λ_{max} (nm)	ref
FA anion	292	this work
FA acid	305	this work
FA acid + anion, pH 5.0	297	this work
DPFATG	306	McFarland and Rojas (1986)
FA-serine [*N*-acetyl-*O*-(β-2-furylacryloyl)serinamide]	309	Charney and Bernhard (1967)
FA-methyl ester	306	Bernhard et al. (1965)
FA-imidazole	353	Bernhard et al. (1965)
FA-cysteine [*N*-acetyl-*S*-(β-2-furylacryloyl)cysteine]	338	Hinkel and Kirsch (1970)
FA-chymotrypsin	320	Bernhard et al. (1965)
FA-LPL	305	this work

References

Bengtsson, G., & Olivecrona, T. (1982) *Biochim. Biophys. Acta 712*, 196–199.

Bernhard, S. A., Lau, S. J., & Noller, H. (1965) *Biochemistry 4*, 1108–1118.

Burdette, R. A., & Quinn, D. M. (1986) *J. Biol. Chem. 261*, 12016–12021.

Charney, E., & Bernhard, S. A. (1967) *J. Am. Chem. Soc. 89*, 2726–2733.

Coll, R. J., Compton, P. D., & Fink, A. L. (1982) *Methods Enzymol. 87*, 66–76.

Hinkel, P. M., & Kirsch, J. F. (1970) *Biochemistry 9*, 4633–4643.

Iverius, P. H., & Ostlund-Lindqvist, A.-M. (1976) *J. Biol. Chem. 251*, 7791–7795.

Iverius, P. H., & Ostlund-Lindqvist, A.-M. (1986) *Methods Enzymol. 129*, 691–704.

Kinnunen, P. K. J. (1977) *Med. Biol. 55*, 187–191.

McFarland, J. T., & Rojas, C. (1986) *Biochim. Biophys. Acta 876*, 438–449.

Olivecrona, T., & Bengtsson, G. (1983) *Biochim. Biophys. Acta 752*, 38–45.

Olivecrona, T., Bengtsson, G., & Osborne, J. C. (1982) *Eur. J. Biochem. 124*, 629–633.

Ostlund-Lindqvist, A.-M. (1979) *Biochem. J. 179*, 555–559.

Parkin, S. M., Speake, B. K., & Robinson, D. S. (1982) *Biochem. J. 207*, 485–495.

Reddy, M. N., Maraganore, J. M., Meredith, S. C., Heinrickson, R. L., & Kezdy, F. J. (1986) *J. Biol. Chem. 261*, 9678–9683.

Schonbaum, G. R., Zerner, B., & Bender, M. L. (1961) *J. Biol. Chem. 236*, 2930–2935.
Sugiura, M. (1984) in *Lipases* (Borgstrom, B., & Brockman, H., Eds.) pp 505–524, Elsevier, Amsterdam.
Vainio, P., Virtanen, J. A., & Kinnunen, P. K. J. (1982) *Biochim. Biophys. Acta 711*, 386–390.
Walsh, C. (1979) *Enzymatic Reaction Mechanisms*, pp 84–86, Freeman, San Francisco.

Structure of the Human Thyroid Peroxidase Gene: Comparison and Relationship to the Human Myeloperoxidase Gene†

Shioko Kimura,*,‡ Young-Sook Hong,‡,§ Tomio Kotani,‖ Sachiya Ohtaki,‖ and Fumitaka Kikkawa‡
Laboratory of Molecular Carcinogenesis, National Cancer Institute, National Institutes of Health, Bethesda, Maryland 20892, and Central Laboratory of Clinical Investigation, Miyazaki Medical College Hospital, Kiyotake, Miyazaki, 889-16, Japan
Received October 31, 1988; Revised Manuscript Received January 26, 1989

ABSTRACT: All exons of the human thyroid peroxidase gene were cloned from phage and cosmid libraries and sequenced, including 2599 base pairs of upstream DNA. The gene contains 17 exons and covers at least 150 kilobase pairs of chromosome 2. The transcription start site was identified by both S1 mapping and primer extension; a typical TATA box was found 25 bases upstream of the putative start site. A comparison of the gene structures of thyroid peroxidase and a granulocyte protein, myeloperoxidase, revealed that the positions of the 3rd through 11th exon–intron junctions in thyroid peroxidase coincide exactly with those of the 2nd through 11th exon–intron junctions in myeloperoxidase except the 7th myeloperoxidase junction, that does not have any counterpart in thyroid peroxidase. The amino acid codon separation pattern in each junction is well conserved between both enzymes. Four exons, unique to thyroid peroxidase, are located at the 3′ end of the gene (exons 13–16), each of which encompasses a different protein module. Three of these modules, representing exons 13, 14, and 15, bear significant similarities to C4b-β2 glycoprotein, the EGF-LDL receptor, and a typical transmembrane domain, respectively. The genes coding for these modules were probably fused to an ancestral peroxidase gene to generate the present thyroid peroxidase gene. The data suggest that intron loss, and/or insertion, and exon shuffling have played important roles in the evolution of the thyroid peroxidase gene.

Thyroid peroxidase (TPO;[1] donor:hydrogen-peroxide oxidoreductase, EC 1.11.1.7) is a membrane-bound hemoprotein which is involved in the biosynthesis of thyroid hormones. It catalyzes both the iodination and the coupling of tyrosines in thyroglobulin to yield thyroxine (T4) and triiodothyronine (T3) (DeGroot & Niepomniszcze, 1977; Nunez, 1980). Human TPO was purified by monoclonal antibody assisted chromatography and appeared to have two bands in the 107-kilodalton region of an SDS–polyacrylamide gel (Czarnocka et al., 1985; Ohtaki et al., 1986). TPO has been shown to be a major component of the thyroid microsomal antigen involved in autoimmune thyroid diseases (Czarnocka et al., 1985; Portmann et al., 1985; Kotani et al., 1986). Recently, the cDNA clone to human TPO has been isolated, and its nucleotide and deduced amino acid sequences have been determined (Kimura et al., 1987; Libert et al., 1987a,b; Magnusson et al., 1987). The evidence for the identity of TPO as the microsomal antigen expressed in patients with autoimmune thyroid diseases was further provided by cDNA cloning (Libert et al., 1987b).

A striking homology was found between human TPO and human myeloperoxidase (MPO; Johnson et al., 1987; Morishita et al., 1987a), indicating that both enzymes are members of the same gene family and evolved from a common ancestral gene (Libert et al., 1987b; Kimura & Ikeda-Saito, 1988). Interestingly, the latter enzyme is expressed in granulocytes and monocytes and plays a major role in the H_2O_2-dependent microbicidal system of neutrophils. The tissue-specific expression patterns and physiological roles of TPO and MPO are quite distinct. Due to the similarities of their cDNAs, we sought to examine the relationships between the structure of both peroxidase genes.

The MPO gene has recently been isolated and sequenced (Morishita et al., 1987b). This gene is about 10 kilobase pairs (kbp) long, contains 12 exons (Morishita et al., 1987b), and is located on human chromosome 17 (Weil et al., 1987; Liang et al., 1987). On the other hand, the human TPO gene has been mapped to chromosome 2 (Kimura et al., 1987; Libert et al., 1987b). In the present report, we describe the cloning and complete exon structure of the human TPO gene. The gene spans over 150 kbp and consists of 17 exons and 16 introns. A comparison of exon–intron junctions between the TPO and MPO (Morishita et al., 1987b) genes revealed that the position of the junctions and the amino acid codon separation patterns of both enzymes are well conserved. In addition, the 3′ portion of the TPO gene has the insertion of four unique gene modules which are not observed in the MPO gene. The possible evolutionary events responsible for the divergences and the conservations of DNA sequence between TPO and MPO genes will be discussed.

Materials and Methods

Cloning and Sequencing of the Human TPO Gene. Total DNA was isolated from a blood donor's lymphocytes by a

† The nucleic acid sequence in this paper has been submitted to GenBank under Accession Number J02856.
‡ National Cancer Institute.
§ Present address: College of Medicine, Ewha Womans University, Seoul, Korea.
‖ Miyazaki Medical College Hospital.

[1] Abbreviations: bp, base pair(s); kbp, kilobase pair(s); TPO, thyroid peroxidase; MPO, myeloperoxidase.

0006-2960/89/0428-4481$01.50/0